

## Magnetic anisotropy energy and interlayer exchange coupling in ultrathin ferromagnets: experiment versus theory

Klaus Baberschke\*

*Institut für Experimentalphysik, Freie Universität Berlin, Arnimallee 14,  
D-14195 Berlin, Germany*

*(Received 8 May 2008; final version received 13 June 2008)*

The study of magnetism and crystallography of nanostructures is one of the most challenging topics, at present. Novel structures were grown, which do not exist in the bulk; the magnetism of these nano-sized particles and films may differ from the bulk by orders of magnitude. Synergistic applications of theory and experiment in materials science are all important for a fundamental understanding. The most important parameters are the magnetic anisotropy energy (MAE) and the interlayer exchange coupling (IEC) in multilayers. We will discuss examples where *ab initio* calculations adapted to existing experiments disentangle the importance of surface and volume effects in the MAE, as well as a layer-resolved IEC and its  $T$ -dependence. The Weinberger group has unambiguously shown that the ‘volume part’ of the MAE is most important to understand the spin reorientation transition (SRT) in Ni/Cu. They also calculated the IEC layer-by-layer in the  $T=0$  limit for a trilayer. Very recently, in theory, spin wave excitations were added to interpret the experimental findings.

**Keywords:** magnetic anisotropy; interlayer exchange; magnetic films

### 1. Introduction

Magnetism has been a fascinating field for a long time. Traditionally two subgroups have been developed: the single-particle magnetism of isolated atoms and molecules and the collective magnetism with ordering phenomena, critical temperature of an ensemble of localized or itinerant magnetic moments. In the first category belong, for example, dilute 3d, 4f ions, but also Cu, Ag, Au atoms in the gas phase; they carry a magnetic moment. In an external magnetic field  $H_0$ , they undergo the Zeeman effect, and various experimental techniques (e.g. optical spectroscopy, paramagnetic resonance, etc.) can be used to measure the orbital and spin part of the magnetic moment per particle. The second category focuses on magnetic order, ferro-, or antiferromagnetism. Here the majority of experiments deal with hysteresis loops, coercive fields, magnetic domains, etc. In this group most of the experimental techniques are limited to temperatures  $T < T_c$ . Spin polarized PE, MOKE, XMCD – they all lose their signal with vanishing magnetization  $M$ . As a matter of fact, a large fraction of the literature calls the regime above  $T_c$  ‘non-magnetic’ instead of ‘paramagnetic’. However both the para- and ferromagnetic

---

\*Email: bab@physik.fu-berlin.de

phases carry the same fingerprint, namely orbital and spin magnetic moments,  $\mu_L$ , and  $\mu_S$ .  $\mu_L$  and its anisotropy is the only origin of magnetic anisotropy energy (beside a dipolar contribution). In both phases, for  $T \geq T_c$ , this is manifested in the tensor components of the g-factor. In the ‘subgroup of ferromagnetism’ various names have been introduced, like magneto-elastic, magnetostriction, magneto-crystalline anisotropy, etc.; they all originate from the same source, the non-vanishing orbital magnetism. Even the so-called anisotropic exchange can be interpreted as hidden orbital magnetism, projected into spin-space. For an isotropic Heisenberg Hamiltonian,  $\mathbf{S}_i \cdot \mathbf{S}_j$  it costs no energy to rotate parallel (or antiparallel) aligned spins in space. Only the orbital angular moment  $\mathbf{L}$ , the non-spherical charge distribution, couples to  $\mathbf{r}$ -space, the crystallographic lattice.

Fert and Levy [1,2] showed, quite early, that an exchange coupling, for example of Mn–Mn pairs in a dilute Mn:Cu alloy, produce no anisotropy; the isotropic exchange interaction cannot explain the field-cooling memory in spin glasses. Only triangle coupling via an impurity, e.g. Pt or Au, creates a ‘missing inversion symmetry’ along the Mn–Mn axis. They calculated this in third-order perturbation theory with dominant spin–orbit interaction at the (Pt or Au) impurity site. They also pointed out that this spin–orbit contribution is the main ingredient in the  $3 \times 3$  matrix of coupling with missing inversion symmetry, i.e. the Dzyakoshinsky–Moriya (DM) interaction. The DM interaction, as discussed at this conference, is the lowest order coupling with missing inversion symmetry for the off-diagonal matrix elements – a unidirectional mechanism. It did explain the memory effect in spin glasses and it will explain the exchange bias at interfaces of nanostructures, today. On today’s level a third-order perturbation theory using Schrödinger’s equation may not be sufficient, in some cases. One might go right away and solve the full Dirac equation. That however, means that we should not use the picture of Pauli particles, but directly the Dirac particles, with the spin not being a good quantum number. In any case, only the orbital magnetism causes anisotropy in magnetism. Without it, we would have no hard magnets and no magnetic storage media.

Most of the experiments do not measure the anisotropy field (or the interlayer exchange field), but rather the energy. That is to say, the product of  $\boldsymbol{\mu} \cdot \mathbf{H}_{\text{an}}$ . Caution must be taken when interpreting these numbers. The magnetic moment at the surface, and at an interface differ significantly from the moment in the inner part of a nanostructure. For example, for a Co/Cu (001) film of several ML thickness, the surface layer, facing vacuum, has an  $\approx 32\%$  enhanced moment. But at the Co–Cu interface the Co moment is  $\approx 17\%$  reduced, due to hybridization effects with Cu [3]. In this article we will not discuss the details of the experiment, but refer to recent publications [4–8].

To calculate the magnetic anisotropy energy (MAE) from *first principle* is a challenge. The difference in energy/particle in different crystallographic directions ranges from  $\mu\text{eV}$  to a few meV, which is a small fraction out of the total energy/atom, being several eV. But, if successful, the theory has great advantages compared to experiments; it can change the crystallographic structure arbitrarily, it allows us to calculate the magnetism layer-by-layer, it can separate orbital and spin magnetism, etc. In the following we will discuss some recent examples in which the theory has adapted realistic experimental conditions. Both together, experiment and theory, serve for a better fundamental understanding of the MAE (Section 2) and the interlayer exchange coupling (IEC) (Section 3) in ferromagnetic nanostructures.

## 2. Magnetic anisotropy energy

The growth of ferromagnetic ultrathin films or nanoparticles opens a completely new variety of crystallographic structures, which do not exist in the bulk. For example, tetragonal Ni can be grown epitaxially on Cu(001), or trigonal Co on Cu(111). The departure from cubic fcc structure may be small and for some aspects of electronic band structure calculations unimportant. In other words, to assume a perfect cubic lattice for Fe, Co, or Ni with the lattice constant of the Cu substrate crystal facilitates numerical calculation and may be sufficient for some aspects in the band structure and DOS, but for magnetism, the  $\mu_L$  and the MAE, it is not. Already a few hundreds of an Å change in the nearest neighbour (n.n.) distance may change the MAE by an order of magnitude. This has been nicely demonstrated by the Uppsala theory group [9]. They assumed an infinite-sized single crystal of Ni, that is to say, no surface effects or hybridization at the interface are considered; the full MAE originates from the inner part of a crystal, the so-called volume part  $K_V$ . The  $c/a$  ratio was changed from fcc with  $c/a = 1$  via tetragonal symmetry to bcc with  $c/a = 1/\sqrt{2}$  – the Bain path (Figure 1a).

In experiment only one value can be realized: pseudomorphic growth of Ni/Cu(001) creates an fct structure (Figure 2a) with  $c/a \approx 0.95$  with  $\epsilon_1 = +2.5\%$  and  $\epsilon_2 = -3.2\%$ . The lateral n.n. distance in bulk Ni equals 2.49 Å, on Cu(001) it is 2.55 Å, a lateral stretching of 0.06 Å, only! In Figure 1(b) we project this value of  $c/a \approx 0.95$  on the theoretical spin-orbit (SO) and SO + orbital polarization (OP) calculation (yellow regime), yielding an MAE of  $K_V \approx 100 \mu\text{eV}/\text{atom}$ , in good agreement with experiment [10]. We conclude that very small distortions in the crystal structure can change the MAE by orders of magnitude *without* employing surface effects, etc. Also in nanostructures and dots, as discussed these days, the crystal structure will depart from the bulk.

In Figure 2(a) also the surface and interface contributions  $K_{S1}$  and  $K_{S2}$  to the MAE are indicated. Their contribution to the total MAE scales down with the increasing number of layers  $d$  (ML) (Néel's argument). In most experiments only the sum of the two is determined:

$$K = K_V + 2K_S/d. \quad (1)$$

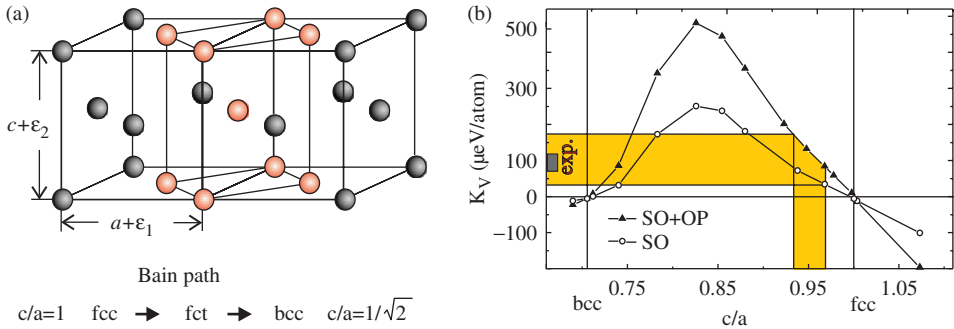


Figure 1. (Colour online) (a) Transformation of an fcc into a bcc structure via the Bain path. (b) *Ab initio* calculation of  $K_V$  for an infinite-sized Ni single crystal, using spin-orbit coupling (open circles), only, and adding orbital polarization (full triangles), also [9].

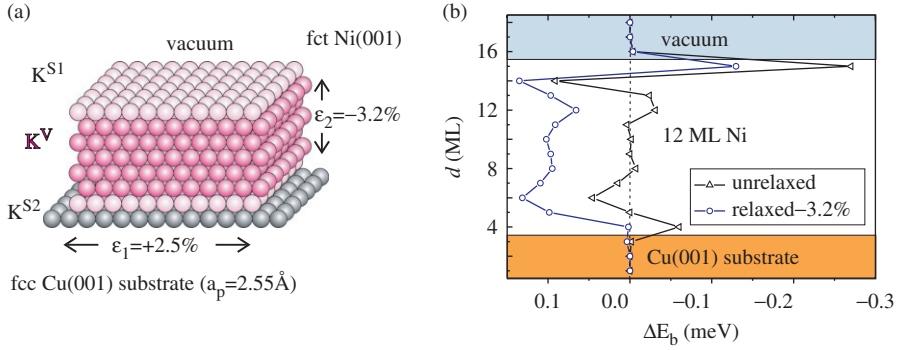


Figure 2. (a) Schematic of ultrathin Ni film pseudomorphically grown on Cu(001). (b) *Ab initio* calculation layer-by-layer of  $K$  (or  $\Delta E_b$ ) [11] (note that the relaxation of  $-5.5\%$  in [11] is normalized to Ni and identical to  $-3.2\%$  normalized to Cu in the present work); see text.

Here we will discuss only the intrinsic contribution  $K$  (or  $\Delta E_b$ ) due to the band structure. For the fct Ni crystal also a second – dipolar – contribution is calculated, but it is very small and will be neglected in the following. In experiments of ultrathin films the dipolar shape anisotropy of  $2\pi M^2$  must be subtracted firstly, before discussing the  $K$ -value of Equation (1).

The Weinberger group has adapted the crystallographic structure of pseudomorphic Ni/Cu(001) and calculated the  $\Delta E_b$  layer-by-layer for several thicknesses of the Ni films [11]. In Figure 2(b) we show the result for 12 ML. It is clear that the surface layer, facing vacuum, carries a large negative anisotropy energy; also the interface layer has a negative contribution. But this affects only one layer each. The inner part of an unrelaxed (cubic) structure shows more or less no large MAE contribution. But if we accept a tetragonally distorted lattice, we see the same result as in the previous paragraph and in Figure 1: each layer contributes  $+\approx 100\mu\text{eV}/\text{layer}$  (open circles in Figure 2b). We conclude: *Surface and interface contributions to the MAE may be large and negative, but count only for one layer each. The inner part of a nanostructure,  $K_V$ , will overcome this, because it counts for  $n-2$  layers.*

Normally experiments cannot measure the MAE layer-by-layer; this can be extracted only from a full set of thickness-dependent measurements. When varying the thickness  $d$  a second problem enters: due to the *finite size effect* also  $T_C(d)$  is a function of thickness (Figure 3a). For example, to measure  $K$  and/or  $M$  as  $f(d)$  only at a fixed (ambient) temperature, this is of very little use; both  $K$  and  $M$  are themselves a function of  $T$ , and even more complicated a function of the reduced temperature  $t = T/T_C$ . Both will vanish at  $T_C$ . Figure 3(b) demonstrates the problem: Gd films at various thicknesses were measured at different reduced temperatures [12]. With such a proper set of experimental data a reliable analysis of  $K(1/d)$  may be performed. Similar results are given for Ni/Cu(001) in Figure 3(c). Taking  $T/T_C(d)$  into consideration, we always find a linear  $1/d$  dependence (Equation 1). Quadratic  $d$ -dependence has been reported in the literature, which indicates changes in the crystal structure and this may produce all kinds of nonlinear  $d$ - and  $T$ -dependences. As long as we are dealing with a given geometrical structure and want to analyse the thickness- and  $T$ -dependence of the MAE, one always expects Equation (1) to be obeyed.

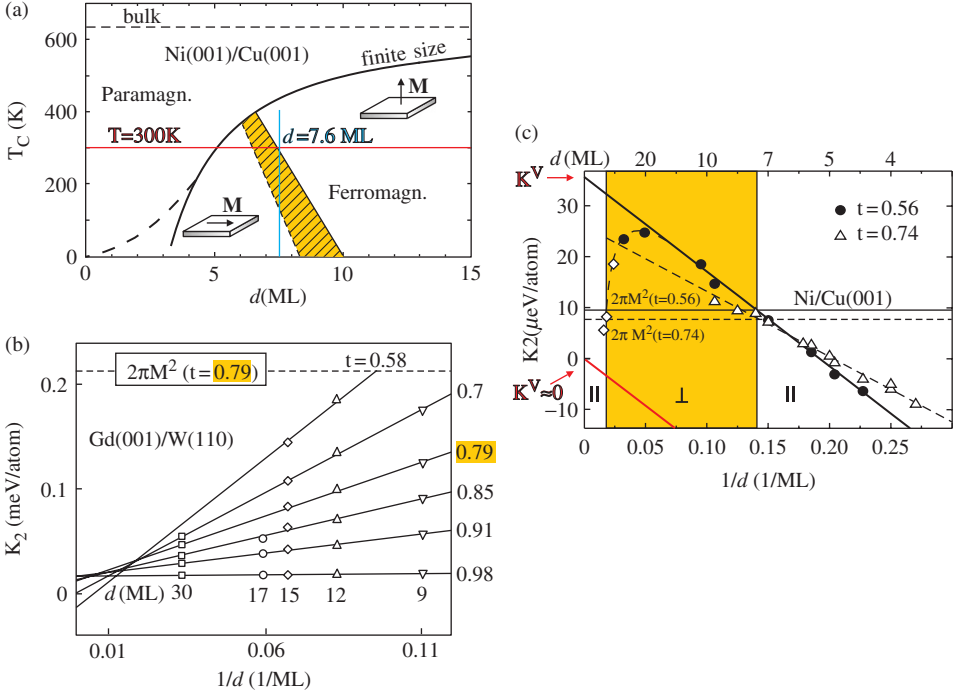


Figure 3. (Colour online) (a) Schematic Curie temperature  $T_C(d)$  for Ni/Cu(001). The solid line indicates the finite size scaling. This is an asymptotic solution for thicker films. Ultrathin films ( $d \leq 4$  ML) depart from this (dashed line) and remain ferromagnetic at low  $T$ . The yellow regime indicates a continuous rotation of the easy axis from in- to out-of-plane [4]. (b) Uniaxial anisotropy for Gd/W(110) as a function of  $1/d$  for different reduced temperatures [12]. (c) Same plot as in (b) for Ni/Cu(001).

Figure 3(c) shows the MAE as a function of  $1/d$  (the dipole contribution is already subtracted from the experimental data). The data range from  $d > 4$  ML to  $d < 20$  ML. If normalized to the specific  $T_C$  at a given  $d$  value, the data obviously follow the linear  $1/d$  dependence. All three contributions,  $K_V$ ,  $K_S$ , and  $2\pi M^2$ , are in the range 10–100  $\mu$ eV/atom, that is to say, surface and volume MAE are the same order of magnitude. Here the physics of the spin reorientation transition (SRT) becomes very transparent:  $K > 2\pi M^2$  favours out-of-plane, but if the dipolar energy wins, in-plane is the easy axis, certainly. So, let's ask the question, Why is there a SRT for Ni, but not for Fe and Co? We see in Figure 3(c) that the dipolar contribution increases quadratically with  $M$ , i.e. for Fe and Co the horizontal  $2\pi M^2$  line moves up by a factor of 8–14 and will never intercept with Equation (1). So, the small magnetic moment of Ni keeps the shape anisotropy low and the positive  $K$ -anisotropy may overcome this. Secondly, what causes the SRT,  $K_V$  or  $K_S$ ? Commonly it is argued in the literature that the surface contribution is responsible. Here we show that this is not the case:  $K_S$  is negative with a negative slope of 100–200  $\mu$ eV/atom, like for many other systems (see next paragraph). But the intercept of  $K(1/d)$  with the  $y$ -axis is important. For bulk fcc Ni  $K_V \approx 0$  (red line) and  $K$  would never exceed  $2\pi M^2$ , assuming the same negative slope. Only the large intercept of  $K_V \approx 35$   $\mu$ eV/atom for the perturbed fct structure moves the linear  $1/d$  dependence up and causes an SRT transition

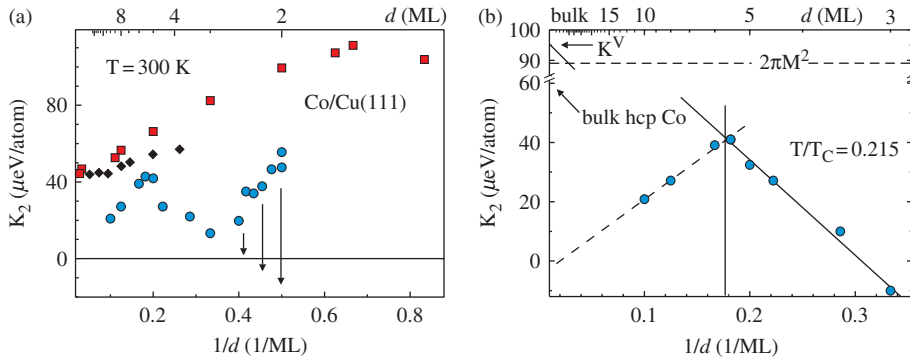


Figure 4. (Colour online) Uniaxial anisotropy for Co/Cu(111) as a function of  $1/d$ , (a) for a fixed temperature of  $T=300$  K and (b) for a constant reduced temperature. Squares and diamonds are taken from [13,14] and circles from [12].

between 7 and 10 ML. Finally, we see at  $\approx 20$  ML the experimental data depart from Equation (1). At this thickness the Ni film ‘remembers’ its bulk fcc structure and the crystal relaxes back to cubic symmetry with a reduced MAE and many misfit dislocations.

Ultrathin Co films on Cu have been investigated by many groups with high intensity. At the beginning of the 1990s the Philips group as well as Gradmann and coworkers measured the uniaxial anisotropy  $K_2$  of Co/Cu(111), shown as diamonds and squares in Figure 4(a) [13,14]. At first glance it looks as if  $K_2$  increases as a function of  $1/d$  with a positive slope. But these data were taken at fixed (ambient) temperature and the thickness dependence of  $T_C$  was ignored. Farle et al. [15] remeasured and plotted the MAE at constant reduced temperature in Figure 4(b). For ultrathin thickness of  $d \leq 6$  ML we see a linear  $1/d$  dependence. In this regime the Co layers grow pseudomorphically on Cu(111). This produces a small trigonal ( $a=b=c$  but  $\alpha=\beta=\gamma \neq \pi/2$ ) distortion in the cubic lattice. If this perturbed cubic structure were to grow up to infinite thickness, the intercept at the  $y$ -axis is about  $K_V \approx 95 \mu\text{eV}/\text{atom}$ . This is very close to the bulk value for hcp Co. In reality the pseudomorphic growth stops at about 6 ML and we turn back to the standard fcc Co with small MAE. The arrows in Figure 4(a) indicate that the data measured at 300 K will move down to negative values, when taking the change of  $T_C(d)$  into account. In summary: *To the best of our knowledge, we find in the literature  $K(d)$  data always following Equation (1). Furthermore we believe, that this type of ‘K-analysis’ is one of the most sensitive techniques to detect small structural changes. It may be more sensitive than LEED or XRD.* If other thickness-dependent behaviour for the MAE is reported (for example quadratic, see e.g. [16]) this will be caused by structural changes as a function of  $d$  or  $T$ . But then, all kinds of functional dependencies may happen, even discontinuities.

Finally, we want to discuss the combined effort of theory and experiment to understand the manipulation of the surface anisotropy  $K_S$ . The Ni/Cu(001) system has been investigated by several groups; it was exposed to H, O, or CO gas [17,18]. These authors reported a shift in the SRT moving from  $\approx 11$  ML to thinner values of about 7 ML, depending on the gas adsorption. In [19] the Ni film was measured, facing vacuum, being capped with Cu, and being grown with oxygen as surfactant. The experimental results are shown in the inset of Figure 5.  $K_2$  follows the linear  $1/d$  dependence in the range of



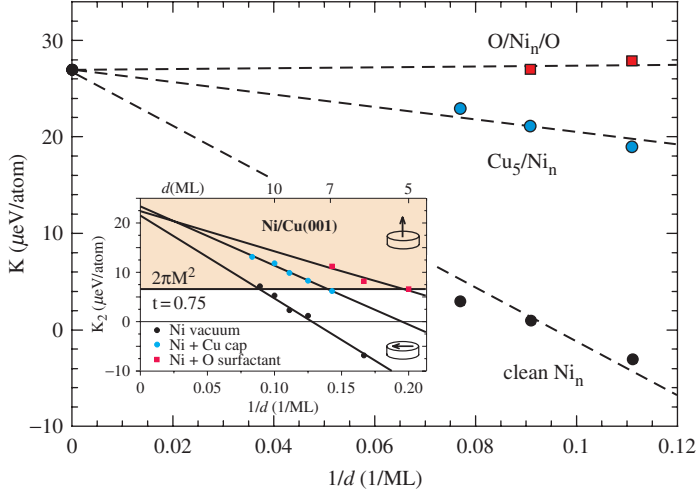


Figure 5. (Colour online) Calculated MAE for clean Ni films, Cu/Ni/Cu superlattices, and Ni films with a  $c(2 \times 2)$  oxygen adlayer [19]. The inset shows the corresponding experiments. For details see text.

5–12 ML with different slopes. That is not surprising; we expect only a change of the surface contribution, and indeed all three lines can be extrapolated to the same intercept on the  $y$ -axis of  $K_V \approx 20\text{--}25 \mu\text{eV}/\text{atom}$ . We also see that the reduction of  $K_S$  is moderate for Cu capping, and the strongest for oxygen surfactant growth. That is explained by Wu and coworker [19] and displayed in Figure 5. They calculated the magnetic anisotropy energy for clean  $\text{Ni}_n$  slabs with both sides vacuum, for  $\text{Cu}/\text{Ni}_n/\text{Cu}$  superlattices, and for a  $c(2 \times 2)$  oxygen adlayer on  $\text{Ni}_n$  films.  $n$  ranges from 5 to 15 layers. For the oxygen surfactant growth the self-consistent calculation results in an outward relaxation of the top Ni layer, and a buckling of the second layer. In principle, this was known from the early research of the Ni surface, but here also the MAE of this layer was calculated and it turned out to be almost zero,  $K_{S1} \approx 0$ . Such a calculation also gives a detailed insight into the electronic band structure and how this is affected by oxygen. There is almost no change in the number of  $d$  electrons in the surface layer, there is no formation of NiO on the surface, but one finds a pronounced antibonding O–Ni peak on top of the Ni  $d$  band, i.e. an O-induced surface state with  $d_{xz}$  character. Its SO splitting is the main feature which reduces  $K_{S1}$ . This combined experimental and theoretical effort, first of all, results in fairly good agreement. Secondly and more important, the calculated spin-dependent electronic band structure can explain what causes what.

### 3. Interlayer exchange coupling and its temperature dependence

The second, equally important, magnetic parameter in ultrathin multilayers is the IEC. This interaction is known to oscillate between ferro- and antiferromagnetic alignment of two ferromagnetic layers, separated by a non-magnetic spacer. A vast number of review papers are available; we refer to the chapters in [8]. When measuring or calculating the free energy, both the MAE and the IEC enter and it is not always easy to disentangle these.

The experimental procedure in FMR measurements opens one way to determine the MAE ( $K$ ) and IEC ( $J_{\text{inter}}^j$ ), separately. In an *in situ* UHV-FMR experiment firstly a single film is measured, and the  $K$ -value determined, then the second FM film is evaporated and the only leftover parameter to be determined is  $J_{\text{inter}}$ , for details see [7]. Usually this is measured at finite temperatures and needs to be extrapolated to  $T=0$ , when comparing with *ab initio* calculations.

Again, the Weinberger group has adapted a realistic experimental situation and calculated  $K^j$  and  $J_{\text{inter}}^j$  layer-by-layer for a prototype system of a  $\text{Ni}_8/\text{Cu}_j/\text{Ni}_9$  trilayer [20]. The results are shown in Figure 6. The  $K$ -values are different for 8 and 9 ML of Ni (Figure 6a and c) and strongly positive when the relaxation of  $-3.2\%$  is taken into account (see Section 2). In Figure 6(b) and (d) the IEC per layer is plotted. First of all, we see that for 3 ML of Cu the IEC is negative (AFM coupling) and positive (FM coupling) for 9 ML, in agreement with experiment. The main contribution to the IEC originates from the first Ni layer at the Ni/Cu interface, but also the adjacent Cu layers contribute – see Figure 6(b). We recall that at a Ni/Cu interface Cu carries an induced magnetic moment. Both Ni and Cu have small but finite orbital moments. This  $\mu_L$  is the source, which couples – via SO interaction – the spin to the crystallographic lattice; we will come back to this. The absolute value of the calculated IEC of approximately  $40\text{--}150\ \mu\text{eV}$  is difficult to compare to experiment, because also the measured value is model dependent. In the analysis of the FMR data a ‘macroscopic’ Heisenberg Hamiltonian is used, and that  $J_{\text{inter}}$  is not the same as a ‘microscopically’ layer-wise calculated IEC in [20].

In earlier review articles  $T=0$  calculations have been compared with experiments measured, let’s say, at room temperature. That may be justified for thicker Fe and Co films, having almost bulk  $T_C$ . For ultrathin films and in particular for Ni one needs to ask the question: What causes the  $T$ -dependence of the IEC; is it mainly an electronic band structure effect, smearing of the Fermi edge, or are spin wave excitations more important,

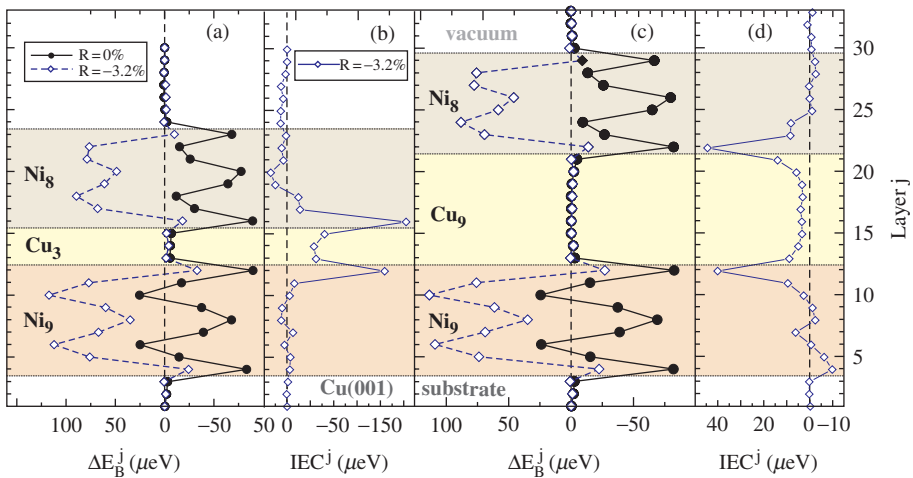


Figure 6. (Colour online) Calculated layer-resolved MAE (or  $\Delta E_b$ ) and IEC for a Ni/Cu/Ni trilayer pseudomorphically grown on a Cu(001) substrate. The number of the Ni layers is fixed to  $j=8$  and  $9$ . The Cu spacer thickness equals  $j=3$  in (a) and (b) and  $j=9$  in (c) and (d). Taken from [20].



which depend on  $T_C$ ? Both theoretical models have been proposed. In [21,22] electronic band structure effects are investigated, leading to a  $T/\sinh(T)$  functional dependence. In [23] magnetic excitations (thermal spin waves) have been discussed as the main source of the  $T$ -dependence of  $J_{\text{inter}}$ . This leads to a power law in reduced temperature  $T/T_C$  with a  $3/2$  exponent. On the other hand, Heinrich recently discussed some experiments [24] and favours a linear  $T$ -dependence. To discriminate between this various analytical functions, experimental data over a large range in temperature are needed. But which  $T$ -range is relevant? The absolute range in kelvin [24] is less relevant. More important seems to us the reduced temperature range, that is to say, to measure from low temperatures up to  $T_C$ . And this is difficult for several ML of Fe and Co. With the highest temperature of 400 K for thicker Fe films [25],  $t = T/T_C$  will be  $\leq 0.4$ . We know only about one experiment [26] in which more or less the full range of reduced temperature was used. These authors measured three different multi- and trilayer systems (Ni/Cu/Co, Ni/Cu/Ni, and an Fe/V multilayer). The reduced temperature covers almost the total range of  $0 < t \leq 0.9$  (Figure 7). Both cases, Figure 7(a) and (b), show an almost perfect power law behaviour with a  $3/2$  exponent. The dashed lines are a simulation of [21,22] with different Fermi velocities. In a more extensive calculation of the band structure effects one should try to use more than one Fermi vector and other details of the Fermi surface. The results in Figure 7 suggest that the spin wave excitations [23] are dominant.

Nolting and coworkers [27] discussed the electronic effects of the  $T$ -dependence in the frame of *ab initio* theory combined with the Fermi liquid model, as well as in the quantum well picture. To treat collective magnetic excitations they used a microscopic Heisenberg model. In addition to the IEC,  $J_{\text{inter}}$ , also a  $J_{\text{intra}}$  is important. This is the exchange coupling within one FM film, a measure also for  $T_C$ . Its realistic values range in the meV regime, whereas  $J_{\text{inter}}$  scales in the  $\mu\text{eV}$  regime. To extract the effect of the magnetic contributions alone for different spacer thicknesses,  $J_{\text{inter}}$  has to be normalized to the parameter  $J_0 \equiv J_{\text{inter}}(T=0)$ . This is shown in Figure 8(a) and (b). In (a)  $J_0$  is constant, and weaker or stronger  $J_{\text{intra}}$  are used. In (b)  $J_{\text{intra}}$  is kept constant, but a gentle  $J_0$  with FM and AFM coupling is used. In all cases Schwieger and Nolting [27] came to the conclusion that  $J_{\text{inter}}(T)$  does not follow an exact  $3/2$  power law – see Figure 8(a) and (b). But one

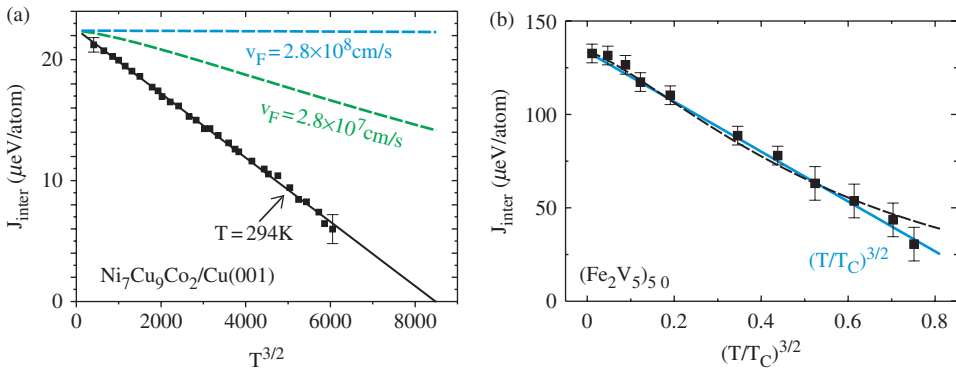


Figure 7. (Colour online)  $J_{\text{inter}}$  as a function of temperature. In (a) the trilayer was measured to  $\approx 400$  K, close to  $T_C$ . In (b) the data for the multilayer are shown as a function of the reduced temperature  $t$ . Taken from [26].

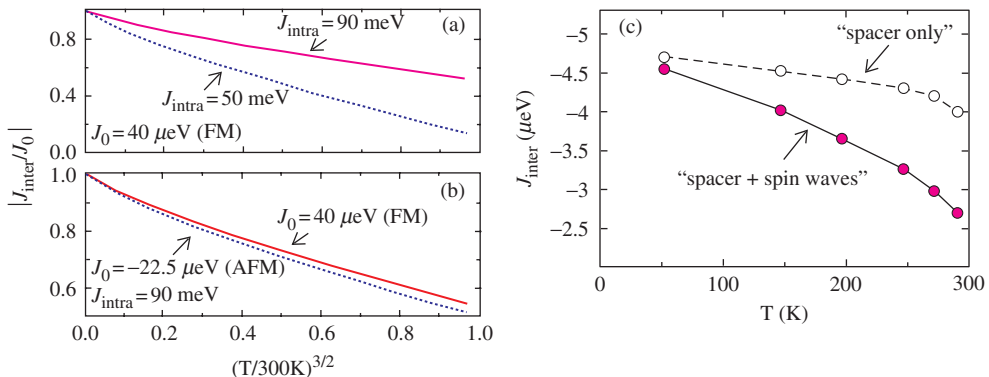


Figure 8. (Colour online)  $J_{\text{inter}}/J_0$  vs.  $T^{3/2}$  for a fixed  $J_0$  in (a) and for fixed  $J_{\text{intra}}$  in (b), from [27]; (c) shows  $J_{\text{inter}}$  as a function of  $T$ , calculated with and without spin wave excitation [28,29].

may want to describe the temperature dependence of the IEC with an ‘effective’ power law with

$$J(T) \approx 1 - AT^n, \quad n \approx 1.5. \quad (2)$$

With this combined theoretical and experimental effect it seems to be evident – and also plausible – that spin wave excitations are the dominant effect for the effective reduction of the IEC at finite  $T$ . Theory has the advantage of switching on and off different mechanisms. That is shown in Figure 8(c); the dashed line shows the reduction of  $J_{\text{inter}}$  by spacer effects only, and the full line with ‘spacer + spin waves’ [28,29].

Recent theoretical investigation, in turn, inspired new FMR experiments [30]. The purpose was to keep the two FM films constant and change only the spacer thickness  $n$ , and observe  $J_{\text{inter}}$  as a function of  $n$ , which should enter into the prefactor  $A$  in Equation (2). What would we expect?

There are three possibilities:

- (1)  $A$  depends only on the interface  $\Rightarrow A(d) = \text{const.}$
- (2)  $A$  depends on electronic band structure  $\Rightarrow A(d) = \text{linear fct.}$
- (3)  $A$  depends on spin waves  $\Rightarrow J_{\text{inter}} \Rightarrow A(d) \approx \text{osc. fct.}$

To answer the question, the Co/Cu/Ni system, with 1.8 ML Co,  $n$  monolayers of Cu spacer, and 7 ML Ni on a Cu (001) substrate was chosen [30]. This work provides for the first time an investigation of the temperature dependence of  $J_{\text{inter}}$  entirely determined from the FMR angular dependence of the ferromagnetic resonance positions at each temperature for the  $n=6$  ML film (Figure 9a). Obviously, the data do not follow a monotonic function of  $d$ , i. e. the slope  $A$  for  $n=4$  fits between  $n=5$  and  $n=6$ . The trend in Figure 9(b) is clear: Large  $J_0$  produces a weak slope  $A$  and vice versa, a very plausible result: *The IEC and the thermal energy  $kT$  are in competition. Very weak  $J_{\text{inter}}$  easily allows thermal excitation of spin wave, and a stronger  $J_{\text{inter}}$  reduces this effect.*

Real interfaces will have steps and other imperfections. For magnetic and non-magnetic ions at these sites the local density of states (DOS) will be different from the bulk, i.e.  $\mu_S$  may change, but more important  $\mu_L$  will increase (see Section 2). For a given

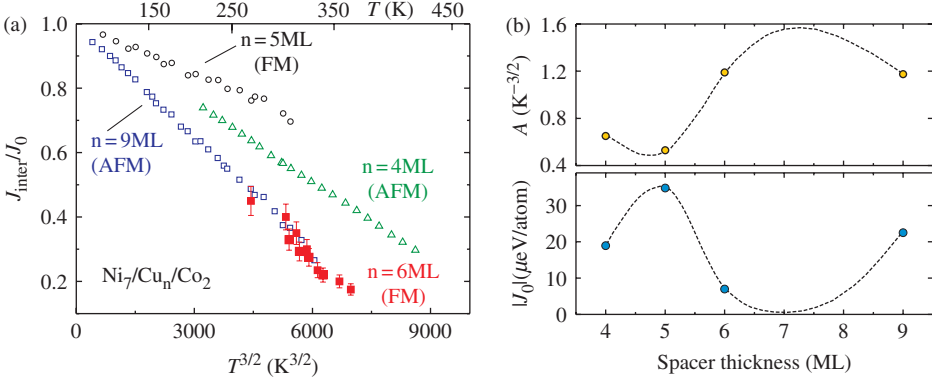


Figure 9. (Colour online) Normalized  $J_{\text{inter}}$  vs.  $T^{1.5}$  for different spacer thickness  $n$ . The data points for the thicknesses of 4, 5 and 9 ML were taken from Schwieger et al. [28,29]; for details see [30].

geometrical arrangement and the corresponding interplay of  $\mu_S$  and  $\mu_L$  this will produce a unidirectional coupling, for example between a FM and AFM film. Such unidirectional coupling leads to what is called ‘exchange bias’. The  $3 \times 3$  matrix of  $J_{\text{inter}}^{ij}$  may have no inversion symmetry, as discussed in [1,2]. Indeed the DM mechanism is employed again to explain ‘unidirectional exchange coupling’ at interfaces.

#### 4. Conclusions

Today’s research on nanomagnetism, storage media, spin injection, etc. is very rich and successful. Many of the experimental findings are interpreted in a simple ‘spin-up, spin-down’ picture, a common procedure in photoemission. The present contribution puts some emphasis on the fact that the orbital magnetic moment and angular momentum are crucial; they are not quenched, they originate the MAE. The anisotropy of  $\mu_L$  is the leading ingredient to create an hysteresis loop with coercive fields. Strictly speaking, not  $S$  but  $J$  is a good quantum number. In the past that has been demonstrated for rare earth spin glasses [31], simulating Ising or XY-systems. In some cases the  $3 \times 3$  coupling matrix between two angular momenta has lower symmetry than uniaxial. This unidirectional mechanism with missing inversion symmetry, the DM interaction, is applicable to explain the ‘exchange bias’ and it was successful in interpreting the field cooling memory effect in spin glasses [1,2]. Finally, we show that for a joint interpretation by theory and experiment in nanomagnetism one must either extrapolate the experimental observables back to  $T=0$ , or include  $T \neq 0$  in the theory. In that case electronic band structure effects, smearing at the Fermi edge, seem to be a minor effect; most important are spin wave excitations and magnon–magnon scattering [32]. In Section 2 we discussed the MAE and the importance of orbital magnetism; in Section 3 thermal spin wave excitations were added to understand  $J_{\text{inter}}(T)$ . Both steps are more or less ‘static arguments’. For a real detailed microscopic understanding we need to consider, in addition, that magnon–magnon scattering, and spin–spin correlations are all important at interfaces of ultrathin ferromagnets. Some experiments and theoretical aspects, that not the static mean field picture but higher order spin correlations control nanomagnetism, are discussed in [33,34].

## Acknowledgements

We are very grateful to the theorists who picked up our experimental findings and helped to form a more fundamental understanding of MAE and IEC in ultrathin ferromagnets. These are the groups of P. Weinberger, O. Eriksson and B. Johansson, D.L. Mills and R. Wu, K.-H. Bennemann and W. Nolting. The experiments would not have been possible without my former coworkers: J. Lindner, K. Lenz, S. S. Kalarickal, E. Kosubek, and X. Xu. In particular E. Kosubek and K. Lenz are acknowledged for assistance in preparing this manuscript. This work was supported in part by BMBF (05KS4 KEB/5) and DFG Sfb 658.

## References

- [1] A. Fert and P. Levy, Phys. Rev. Lett. 44 (1980) p.1538.
- [2] P. Levy and A. Fert, Phys. Rev. B 23 (1981) p.4667.
- [3] A. Ney, P. Pouloupoulos and K. Baberschke, Europhys. Lett. 54 (2001) p.820.
- [4] M. Farle, B. Mirwald-Schulz, A. Anisimov et al., Phys. Rev. B 55 (1997) p.3708.
- [5] K. Baberschke and M. Farle, J. Appl. Phys. 81 (1997) p.5038.
- [6] A.N. Anisimov, M. Farle, P. Pouloupoulos et al., Phys. Rev. Lett. 82 (1999) p.2390.
- [7] J. Lindner and K. Baberschke, J. Phys.: Condens. Matter 15 (2003) p.R193 and S465.
- [8] K. Baberschke, *Investigation of Ultrathin Ferromagnetic Films by Magnetic Resonance*, in *Handbook of Magnetism and Advanced Magnetic Materials*, Vol. 3, Helmut Kronmüller and Stuart Parkin, eds., John Wiley, New York, 2007, p.1617.
- [9] O. Hjortstam, K. Baberschke, J.M. Wills et al., Phys. Rev. B 55 (1997) p.15026.
- [10] B. Schulz and K. Baberschke, Phys. Rev. B 50 (13) (1994) p.467.
- [11] C. Uiberacker, J. Zabloudil, P. Weinberger et al., Phys. Rev. Lett. 82 (1999) p.1289.
- [12] M. Farle, Rep. Prog. Phys. 61 (1998) p.755.
- [13] J. Kohlhepp, H.J. Elmers and U. Gradmann, J. Magn. Magn. Mater. 121 (1993) p.487.
- [14] F.J.A. den Broeder, W. Hoving and P.J.H. Bloemen, J. Magn. Magn. Mater. 191 (1991) p.562.
- [15] M. Farle, W. Platow, E. Kosubek et al., Surf. Sci. 439 (1999) p.146.
- [16] C.A.F. Vaz, J.A.C. Bland and G. Lauhoff, Rep. Prog. Phys. 71 (2008) p.56501.
- [17] R. Vollmer, Th. Gutjahr-Loser, J. Kirschner et al., Phys. Rev. B 60 (1999) p.6277.
- [18] S. van Dijken, R. Vollmer, B. Poelsma et al., J. Magn. Magn. Mater. 210 (2000) p.316.
- [19] J. Hong, R.Q. Wu, J. Lindner et al., Phys. Rev. Lett. 92 (2004) p.147202.
- [20] R. Hammerling, J. Zabloudil, P. Weinberger et al., Phys. Rev. B 68 (2003) p.092406.
- [21] P. Bruno, Phys. Rev. B 52 (1995) p.411.
- [22] V. Drchal, J. Kudrnovsky, P. Bruno et al., Phys. Rev. B 60 (1999) p.9588.
- [23] N.S. Almeida, D.L. Mills and M. Teitelman, Phys. Rev. Lett. 75 (1995) p.733.
- [24] B. Heinrich, in *Magnetic Heterostructures*, Springer Tracts of Modern Physics, Vol. 227, H. Zabel and S.D. Bader, eds., Springer-Verlag, Berlin, 2008, p.185.
- [25] Z. Celisnki, B. Heinrich and J.F. Cochran, J. Magn. Magn. Mater. 145 (1995) p.L1.
- [26] J. Lindner, C. Rüdt, E. Kosubek et al., Phys. Rev. Lett. 88 (2002) p.167206.
- [27] S. Schwieger and W. Nolting, Phys. Rev. B 69 (2004) p.224413.
- [28] S. Schwieger, J. Kienert, K. Lenz et al., Phys. Rev. Lett. 98 (2007) p.057205.
- [29] S. Schwieger, J. Kienert, K. Lenz et al., J. Magn. Magn. Mater. 310 (2007) p.2301.
- [30] S.S. Kalarickal, X. Xu, K. Lenz et al., Phys. Rev. B 75 (2007) p.224429.
- [31] K. Baberschke, P. Pureur, A. Fert et al., Phys. Rev. B 29 (1984) p.4999.
- [32] J. Lindner, K. Lenz, E. Kosubek et al., Phys. Rev. B 68 (2003) p.060102(R).
- [33] K. Baberschke, Physica status solidi (b) 245 (2008) p.174.
- [34] L. Bergqvist and O. Eriksson, J. Phys.: Cond. Matter 18 (2006) p.4853.